

Comparison of Hydroxyapatite Coatings Produced Different Powder Morphology

¹Garip ERDOGAN*, ²Fatih USTEL^b, ¹Ahmet TÜRKA

¹ Metallurgical and Materials Engineering Dept., Manisa Celal Bayar University, Manisa, TURKEY

² Metallurgical and Materials Engineering Dept., Sakarya University, Sakarya, TURKEY

Abstract

Metallic biomaterials are attractive materials for application orthopaedic implants because of their significant mechanical properties. However, metallic biomaterials are generally biocompatible and are required to coat with osteoconductive coatings such as hydroxyapatite (HA) that is natural mineral found in bone tissue. Hydroxyapatite (HA), formulated as $\text{Ca}_{10}(\text{PO}_4)_6(\text{OH})_2$, which has a great osteoconductivity properties with human organism and formed an inorganic part of the bone is used as a biomaterial to repair hard tissues and their configurations. Different methods such as plasma spraying, High velocity oxy-fuel (HVOF), laser, electrophoresis, dip coating, sol-gel methods are widely used to coat the metallic implant materials. On one hand plasma spraying is the most common and economical method for industrial applications, on the other hand, high process temperature of plasma spraying causes defects on HA structure and occurrence of secondary phases. The main effect on the decomposition of HA during spraying is affected by the main process parameters such as plasma gases, process voltage and current and feedstock materials. In this study, HA powders having different size distribution and morphology were used to compare their response for decomposition process. Furthermore, different plasma spray systems were utilized to compare coating structure after spraying. Coating were fabricated grade 5 titanium alloy and coatings were analysed using Scanning Electron Microscope and X-Ray Diffraction methods.

Keywords: Hydroxyapatite coating, powder morphology, plasma spraying

1. Introduction

The development and use of metallic implants have been increased by the demands for bone repair, such as internal fracture fixation of long bones or dental implants to replace a loss or infected tooth. Metallic materials have been used dominantly for orthopaedic including temporary devices such as bone plates and screws [1]. Currently metallic materials have found application for dental application including orthodontic applications dental fillings. However metallic materials are need to be biocompatible, therefore some of the metallic materials such as titanium, cobalt, chromium and iron and their alloys are being used as implant materials [2]. Adhesion of implant and bone tissue also are taken into consideration for improving the metallic biomaterials' response in the living body. In order to increase the adhesion of the metallic implants, coatings such as electrodeposition, thermal spraying, sol-gel are applied on to implant materials [2-4].

Thermal spray is one of the mostly used coating process for orthopaedic implants to coat calcium phosphate based powders. [5,6]. Hydroxyapatite found in naturally bones and dental enamels, which is a calcium phosphate based ceramic, is used to coat metallic implant surface

* Corresponding author: Address: Faculty of Engineering, Department of Metallurgical and Materials Engineering Manisa Celal Bayar University, 45140, Manisa TURKEY. E-mail address: g.erdogan@cbu.edu.tr, Phone: +902362012418

in order to increase biocompatibility of metallic implant and to decrease recovery time of the patient [7–9]. Spraying HA powders with plasma spraying have found many commercial applications because of high deposition and porosity rates. However, high temperature during plasma spraying, which is the nature of the process, leads to decomposition of HA powders into different phases such as tetra calcium phosphate, tricalcium phosphate etc. and amorphous HA[10–12]. Decomposed phases exhibit different solubility in vivo condition and therefore decomposition of HA should be controlled during spraying. Different approaches proposed to control the decomposition during plasma spraying of HA with low plasma power or different plasma gases. In this work, two different commercially available plasma generators and feedstock powder size distribution were used to compare the decomposition of HA powder. Produced coating were analysed using XRD, SEM.

2. Materials and Method

Size distribution of commercially available feedstock powders (Biotal, Captal, UK) were determined by laser diffraction (Microtrack S3500, USA) method. SEM micrographs and size distribution results of the HA powders are shown in Fig.1. In order to spray the HA powders two different plasma generators (Triplex Pro 200 and F4 MB, Oerlikon Metco, Switzerland) were implemented and spraying parameters are given in Table 1. The special configuration Triple cathode design of plasma generator allows using higher voltage amount and it is not suitable to run with hydrogen plasma gas therefore plasma spraying parameters were set to obtain the same amount of energy to avoid the overheating the particles during spraying and prevent the excessive decomposition. Produced coating were metallographically prepared prior to microstructural examination. Scanning Electron Microscope (SEM) was used for microstructural investigation. Samples were heat treated at 600°C for 1hour to eliminate the amorphous phase in the coating structure and X – Ray diffraction analysis (XRD) were implemented to analyse the coating structure before and after heat treatment.

Table 1. Spraying Parameters

| Sample Number | Powder | Gun Type | Primary Plasma Gas [NLPM] | Secondary Plasma Gas [NLPM] | Current [A] | Voltage [V] |
|---------------|------------------|----------------|---------------------------|-----------------------------|-------------|-------------|
| 1 | Spherical Powder | Single Cathode | Argon 55 | Hydrogen 8.8 | 510 | 75 |
| 2 | Angular Powder | Single Cathode | Argon 55 | Hydrogen 8.8 | 510 | 75 |
| 3 | Spherical Powder | Triple Cathode | Helium 80 | Argon 40 | 350 | 110 |
| 4 | Angular Powder | Triple Cathode | Helium 80 | Argon 40 | 350 | 110 |

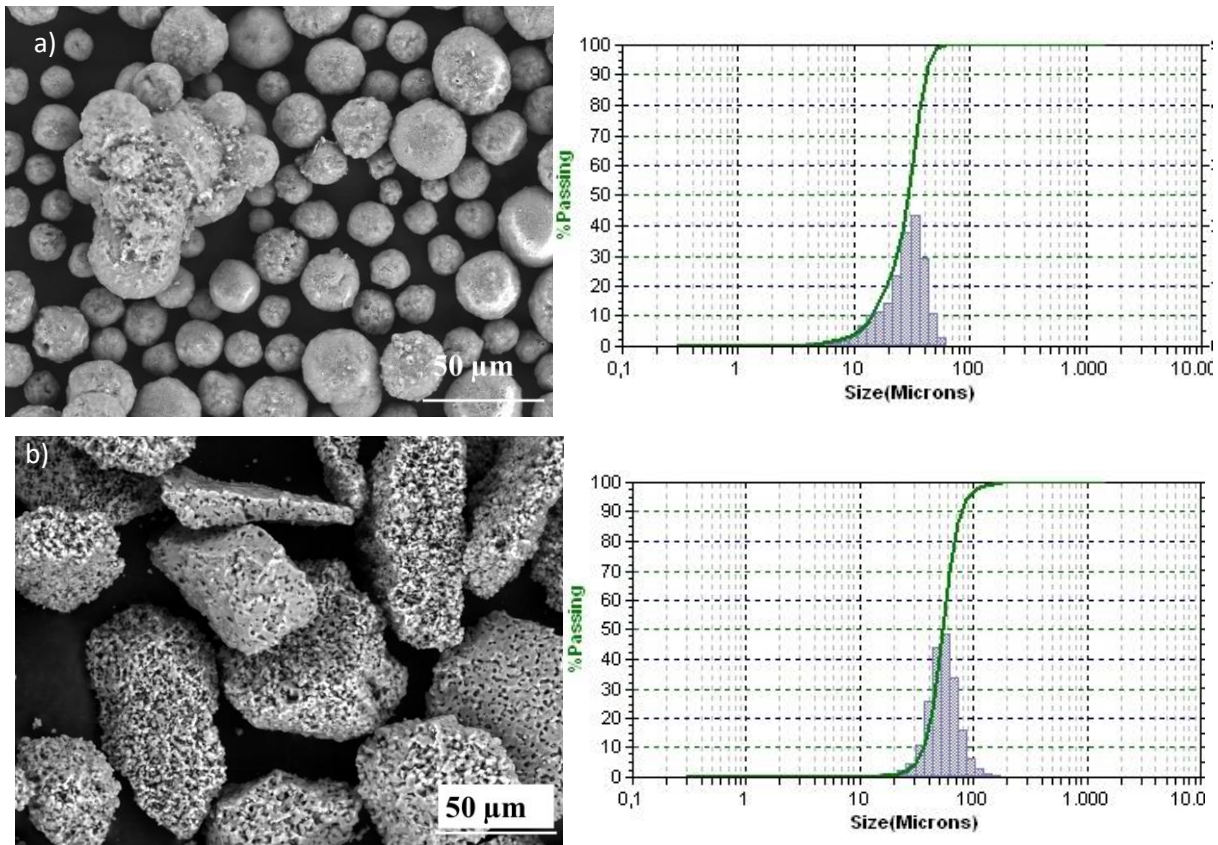


Figure 1 SEM Micrographs of the feedstock particles a) Particle size distribution $d_{50}= 30\mu\text{m}$ b) Particle size distribution $d_{50}= 60\mu\text{m}$

3. Results

It was observed from the SEM images of the feedstock particles that the spherical morphology powder was denser than angular particles. Angular particles consisted of smaller particles as compared to the spherical powder. In fact, both powders consisted of smaller particles but angular shaped powder showed less sintering of the small particles and gives them structural stability during spraying [13–15]. XRD analysis of the feedstock powders (Figure 2.) showed that both powders consist of HA according to PDF card 9-432 and showed similar pattern.

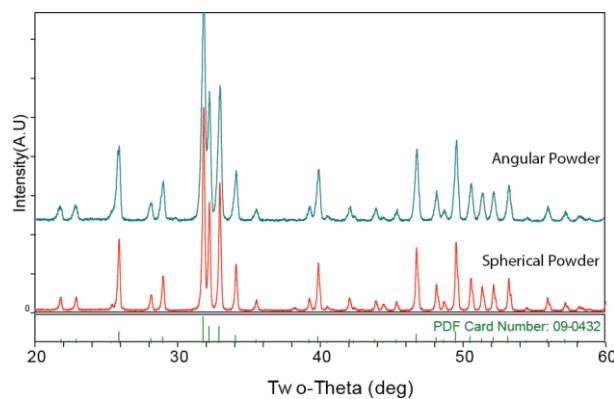


Figure 2. XRD analysis pattern of the feedstock.

SEM micrographs of Sample 1 and Sample 2 are given in Figure 3 and showed that using the same plasma generator with different powder morphology and size distribution the coating structure did not change significantly. The interface between substrate and coating was observed without important delamination and bonding imperfections. Porosity and solidification cracks was observed along the coating structure which was expected due to the plasma spraying nature[14,16,17]. Porosity and surface microcracks of HA coating plays a vital role in living body to increase the adhesion between and bone tissue. Therefore, microcracks could be useful in terms of adhesion of HA coating to the bone tissue. However excessive amount of microcracks decrease the coating mechanical stability and structural integrity[18,19]. Same observation could be seen Figure 4 using triple cathode configured plasma generator, coating structure did not change significantly depending on the powder morphology. Nevertheless, when plasma generators compared in terms of findings from Fig. 3 and Fig. 4, microstructure of the coating changed slightly by lower microcracks and porosity formation. This observation could be attributed to the plasma gas flow ratio.

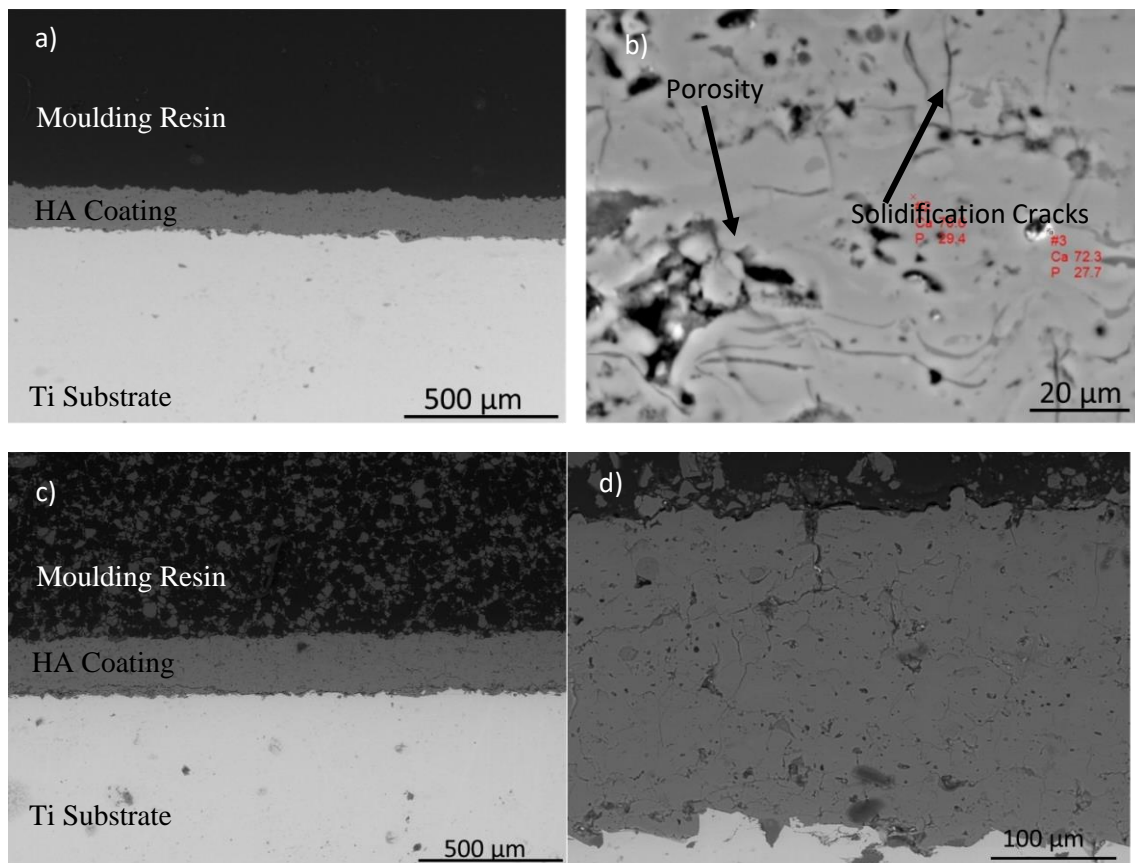


Figure 3. SEM Micrographs a) overall view of Sample 1 b) higher magnification of the Sample 1 c) overall view of Sample 2 d) higher magnification of the Sample 2.

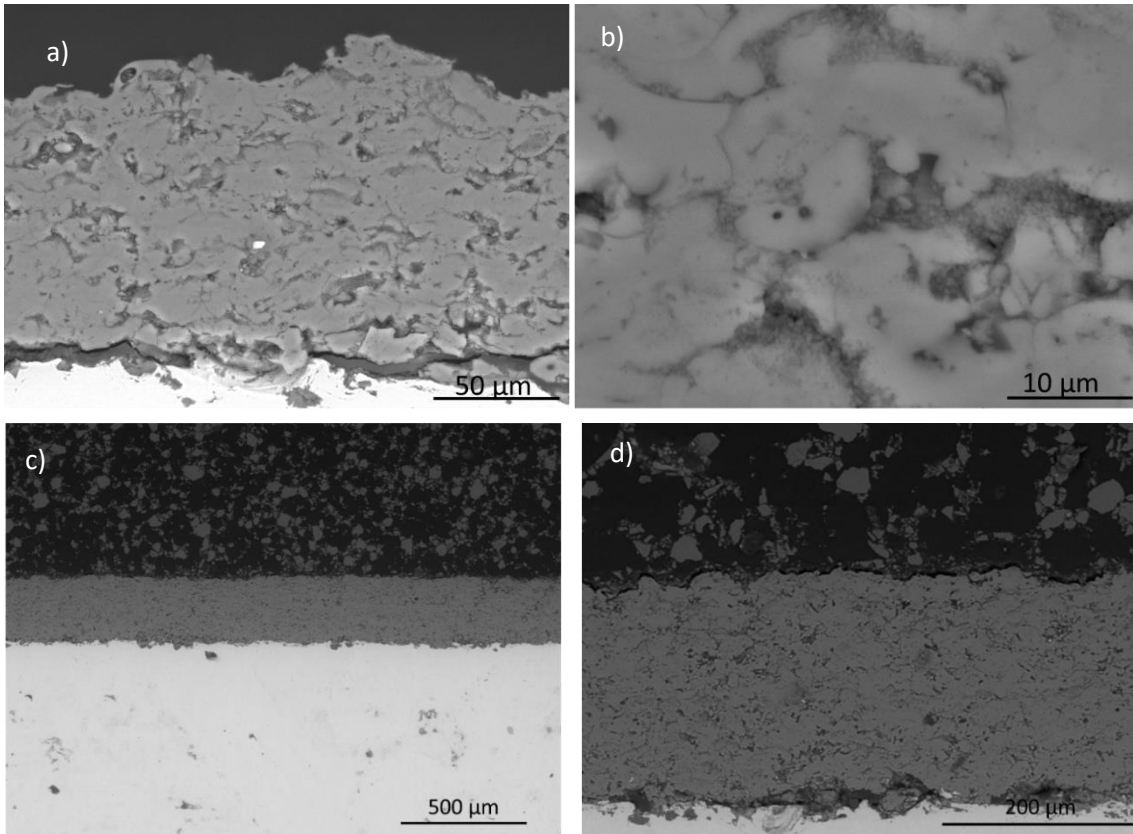


Figure 4. SEM Micrographs a) general view of Sample 3 b) higher magnification of Sample 3. c) general view of Sample 4 d) higher magnification of Sample 4.

XRD analysis results of as sprayed samples are given in Fig. 5. Coating produced with single cathode plasma generator (Sample 1 and 2) showed a decomposition after deposition (Fig. 5a) but coating structure mainly consisted of HA phase. As it could be seen from the magnified view of first sample’s XRD analysis pattern (Fig. 5.b) coating structure decomposed to amorphous (ACP) and whitlockite phase (TCP) that is a calcium phosphate based bio ceramic with chemical formula $Ca_3(PO_4)_2$

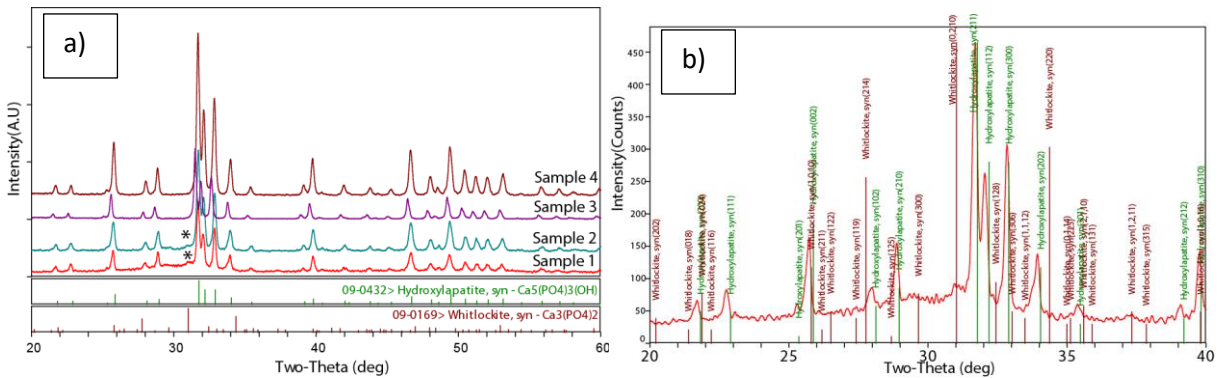


Figure 5. XRD analysis results of as spraying coating a) all samples between XRD pattern 20-60° b) First sample XRD pattern between 20-40°

Fig 6 shows that the samples annealed at 600°C for 1 hour XRD results. After heat treatment decomposed Sample 1 and Sample 2 recovered to the original state. Surprisingly, sample 3 and sample 4 showed decomposition after annealing process a hump right side at main peak became visible matching with whitlockite phase's main peak. Before annealing process, sample 1 and sample 2 showed a ACP phase but the other coatings did not show any amorphous broadening on the XRD pattern.

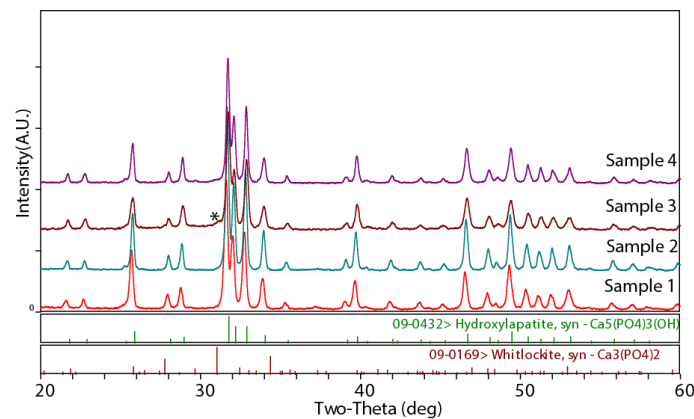
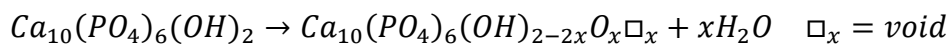


Figure 6 XRD analysis results of as spraying coating a) all samples between XRD pattern 20-60° b) First sample XRD pattern between 20-40°

4. Discussion

Microstructural investigations revealed that having higher plasma gas flow with triple cathode designed compared to single cathode plasma generator allowed higher plasma jet velocity resulting less time to heat flow and fewer microcrack formation[20,21]. High particle velocity played important factor on the porosity formation as well. These results could be useful in terms of decomposition of HA particles due to the fact that low heat input to the HA particle during spraying.

It is well known from the literature [11,20,22,23] that decomposition of HA takes place first oxyhydroxyapatite structure which is similar to HA with a \square_x void formation in the crystal structure and the reaction is given with following the formula;



According to Heimann [24]oxyhydroxyapatite structure is similar to the HA structure therefore XRD pattern is similar to the HA pattern.

XRD analysis revealed that using coarse feedstock particle coating phase structure consisted of less amount of ACP phase. This condition could be seen from Fig.5a with less hump between 20-30 for the sample 2. Despite the coating produced with single cathode plasma generator, the coatings produced with triple cathode plasma generator did not show any decomposition after spraying. Using high amount of plasma gas flow resulted no decomposition in the coating structure. This result, as well, agreed with microstructural investigation.

Conclusion

HA coatings were produced successfully with different feedstock powders and plasma generators. Coatings showed typical plasma sprayed microstructure and coating microstructure did not change with the starting powders. However, using different plasma generator and plasma gases coating microstructure changed having less microcracks. From the XRD analysis coating produced with coarse particle showed less ACP phase. The coatings produced with triple cathode plasma generator did not show any significant decomposition but after heat treatment new peaks appeared indication that first step of decomposition. Further studies should be carried out to point the oxyhydroxapatite formation with high amount of plasma gases during spraying.

References

- [1] Park JB. Bioceramics properties, characterizations, and applications. New York: Springer; 2008.
- [2] Onoki T. Porous Apatite Coating on Various Titanium Metallic Materials via Low Temperature Processing. In: Pignatello R, editor. Biomater. Sci. Eng., InTech; 2011.
- [3] Anselme K. Osteoblast adhesion on biomaterials. Biomaterials 2000;21:667–81. doi:10.1016/S0142-9612(99)00242-2.
- [4] Burdick JA, Mauck RL, editors. Biomaterials for Tissue Engineering Applications. Vienna: Springer Vienna; 2011.
- [5] Brown SR. Characterisation of thermal sprayed hydroxyapatite coatings for use as a biological attachment system for prosthetic devices. Ph.D. Thesis. University of Bath, 1996.
- [6] Chou B-Y, Chang E. Plasma-sprayed hydroxyapatite coating on titanium alloy with ZrO₂ second phase and ZrO₂ intermediate layer. Surf Coat Technol 2002;153:84–92. doi:10.1016/S0257-8972(01)01532-8.
- [7] Akao M, Aoki H, Kato K. Mechanical properties of sintered hydroxyapatite for prosthetic applications. J Mater Sci 1981;16:809–12. doi:10.1007/BF02402799.
- [8] Ben-Nissan B, editor. Advances in Calcium Phosphate Biomaterials. vol. 2. Berlin, Heidelberg: Springer Berlin Heidelberg; 2014.
- [9] Brown PW. Calcium Phosphates in Biomedical Engineering. In: Veyssi re KHJBWCCFIJKM, editor. Encycl. Mater. Sci. Technol. Second Ed., Oxford: Elsevier; 2001, p. 893–7.
- [10] Liao C-J, Lin F-H, Chen K-S, Sun J-S. Thermal decomposition and reconstitution of hydroxyapatite in air atmosphere. Biomaterials 1999;20:1807–13. doi:10.1016/S0142-9612(99)00076-9.
- [11] Ou S-F, Chiou S-Y, Ou K-L. Phase transformation on hydroxyapatite decomposition. Ceram Int 2013;39:3809–16. doi:10.1016/j.ceramint.2012.10.221.
- [12] Heimann RB, Wirth R. Formation and transformation of amorphous calcium phosphates on titanium alloy surfaces during atmospheric plasma spraying and their subsequent in vitro performance. Biomaterials 2006;27:823–31. doi:10.1016/j.biomaterials.2005.06.029.
- [13] Khor KA, Cheang P. Plasma sprayed hydroxyapatite(HA) coatings produced with flame spheroidised powders. J Mater Process Technol 1997;63:271–6. doi:10.1016/S0924-0136(96)02634-9.

- [14] Cheang P, Khor KA. Thermal spraying of hydroxyapatite (HA) coatings: Effects of powder feedstock. *J Mater Process Technol* 1995;48:429–36. doi:10.1016/0924-0136(94)01679-U.
- [15] Fu L, Aik Khor K, Peng Lim J. The evaluation of powder processing on microstructure and mechanical properties of hydroxyapatite (HA)/yttria stabilized zirconia (YSZ) composite coatings. *Surf Coat Technol* 2001;140:263–8. doi:10.1016/S0257-8972(01)01168-9.
- [16] Li H, Khor K a., Chow V, Cheang P. Nanostructural characteristics, mechanical properties, and osteoblast response of spark plasma sintered hydroxyapatite. *J Biomed Mater Res A* 2007;82A:296–303. doi:10.1002/jbm.a.31143.
- [17] Sun L, Berndt CC, Khor KA, Cheang HN, Gross KA. Surface characteristics and dissolution behavior of plasma-sprayed hydroxyapatite coating. *J Biomed Mater Res* 2002;62:228–236. doi:10.1002/jbm.10315.
- [18] Gross KA, Ray N, Røkkum M. The contribution of coating microstructure to degradation and particle release in hydroxyapatite coated prostheses. *J Biomed Mater Res* 2002;63:106–14. doi:10.1002/jbm.10090.
- [19] Laonapakul T, Rakngarm Nimkerdphol A, Otsuka Y, Mutoh Y. Failure behavior of plasma-sprayed HAp coating on commercially pure titanium substrate in simulated body fluid (SBF) under bending load. *J Mech Behav Biomed Mater* 2012;15:153–66. doi:10.1016/j.jmbbm.2012.05.017.
- [20] Cizek J, Khor KA. Role of in-flight temperature and velocity of powder particles on plasma sprayed hydroxyapatite coating characteristics. *Surf Coat Technol* 2012;206:2181–91. doi:10.1016/j.surfcoat.2011.09.058.
- [21] Cizek J, Khor KA, Prochazka Z. Influence of spraying conditions on thermal and velocity properties of plasma sprayed hydroxyapatite. *Mater Sci Eng C* 2007;27:340–4. doi:10.1016/j.msec.2006.05.002.
- [22] Heimann RB. Thermal spraying of biomaterials. *Surf Coat Technol* 2006;201:2012–9. doi:10.1016/j.surfcoat.2006.04.052.
- [23] Gross KA, Berndt CC. Thermal spraying of hydroxyapatite for bioceramic applications. *Key Eng. Mater.*, vol. 53, 1991, p. 159–165.
- [24] Heimann RB. Structure, properties, and biomedical performance of osteoconductive bioceramic coatings. *Surf Coat Technol* 2013;233:27–38. doi:10.1016/j.surfcoat.2012.11.013.